Korean J. Chem. Eng., 35(1), 99-109 (2018)
DOI: 10.1007/s11814-017-0238-3

pISSN: 0256-1115
eISSN: 1975-7220

Selective transformation of biomass-derived 5-hydroxymethylfurfural into 2,5-dihydroxymethylfuran via catalytic transfer hydrogenation over magnetic zirconium hydroxides

Lei Hu†, Mei Yang, Ning Xu, Jiaxing Xu, Shouyong Zhou, Xiaozhong Chu, and Yijiang Zhao

Jiangsu Key Laboratory for Biomass-based Energy and Enzyme Technology, School of Chemistry and Chemical Engineering, Jiangsu Collaborative Innovation Center of Regional Modern Agriculture & Environmental Protection, Huaiyin Normal University, Huaian 223300, China
(*Received 18 July 2017 • accepted 22 August 2017*)

Abstract−An economical and effective approach for the selective transformation of biomass-derived 5-hydroxymethylfurfural (HMF) into 2,5-dihydroxymethylfuran (DHMF) was developed by catalytic transfer hydrogenation over various magnetic zirconium hydroxides (MZHs). As expected, MZH with a moderate Zr/Fe molar ratio of 2 displayed the highest catalytic activity, resulting in 98.4% HMF conversion and 89.6% DHMF yield at 150 °C for 5 h in the presence of 2-butanol that simultaneously acted as the hydrogen donor and reaction solvent, which was ascribed to its appropriate specific surface area, pore size and acid-base content. Moreover, a plausible reaction mechanism for the catalytic transfer hydrogenation of HMF into DHMF over MHZ(Zr/Fe=2) was also proposed, in which the basic hydroxyl groups with the aid of acidic zirconium metal centers were considered to be responsible for the pivotal hydride transfer via a six-membered ring structure.

Keywords: 5-Hydroxymethylfurfural, 2,5-Dihydroxymethylfuran, 2-Butanol, Catalytic Transfer Hydrogenation, Magnetic Zirconium Hydroxides

INTRODUCTION

In recent years, with the continuous depletion of fossil resources and the incessant deterioration by environmental pollutions, the increasing research interest has been concentrated on the conversion of renewable biomass resources into various valuable chemicals in a much more sustainable way [1-5]. 5-Hydroxymethylfurfural, which can be produced by the dehydration of biomass-derived carbohydrates such as fructose, glucose, sucrose, maltose, cellobiose, inulin, starch and cellulose, is considered to be one of the most important platform molecules [6-10]. This is because it can be used as a versatile intermediate for the synthesis of a series of high value-added derivatives such as 2,5-dihydroxymethylfuran (DHMF) [11], 2,5-dimethylfuran (DMF) [12], 2,5-dihydroxymethyltetrahydrofuran (DHMTHF) [13], 1,2,6-hexanetriol (HTO) [14], 2,5-diformylfuran (DFF) [15], 2,5-furandicarboxylic acid (FDCA) [16], 5-ethoxymethylfurfural (EMF) [17], 5-arylaminomethyl-2-furanmethanol (AAMFM) [18], 1-hydroxyhexane-2,5-dione (HHD) [19], 5,5′-bis(hydroxymethyl)furoin (BHMF) [20], 5,5′-oxy-(bismethylene)-2-furaldehyde (OBMF) [21] and furfuryl alcohol (FFA) [22]. Among the above-mentioned derivatives, DHMF which is prepared by the selective hydrogenation of HMF is particularly attractive, which is because DHMF has a special symmetrical structure and tremendous application potential in the production of resins [23], fibers [24], foams [25], drugs [26], polymers [27-29] and crown ethers [30-32].

HMF has three functional groups, including an aldehyde group, a hydroxyl group and a furan ring. Hence, it shows a very strong chemical reactivity [33]; how to ensure the hydrogenation priority of aldehyde group and avoid the further hydrogenolysis of hydroxyl group and furan ring are the key issues in the selective transformation of HMF into DHMF. To solve these issues, designing an appropriate catalytic system is especially significant. Up to now, most conventional catalytic systems for the selective transformation of HMF into DHMF are mainly composed of precious metal catalysts (such as Ru/C [34], Ru/ZrO_2 [35], Ru/CeO_x [36], Ru/MSZN [37], Pt/C [38], Pt/Al_2O_3 [31], Pt/MCM-41 [39], Au/FeO_x [40], Au/Al_2O_3 [41], Ir/TiO_2 [42] and $Ir\text{-}ReO_x/SiO_2$ [43]) and molecular hydrogen (H_2) [34-43]. Although excellent results have been achieved, these conventional catalytic systems possess a serious deficiency, which is that precious metal catalysts and H_2 are extremely expensive. From the perspective of practical production, it is uneconomic for the selective transformation of HMF into DHMF by using the above conventional catalytic systems. More recently, some new catalytic systems have also been employed for the selective transformation of HMF into DHMF via disproportionation reaction [44-46], electrocatalytic method [47-49], photocatalytic method [50] and biocatalytic method [51], which can be performed over non-precious metal catalysts (such as Na-, Fe-, Ni-, Zn- and Al-based catalysts) without the need of external H_2. However, the treatment of corrosive alkali, the lower faradaic efficiency, negligible product yield and the longer reaction time are their unavoidable demerits, respec-

†To whom correspondence should be addressed.
E-mail: hulei@hytc.edu.cn
Copyright by The Korean Institute of Chemical Engineers.

tively. Thus, exploring an economical and effective catalytic system is very necessary and desirable for the selective transformation of HMF into DHMF.

Meerwein-Ponndorf-Verley (MPV) reaction, a typical catalytic transfer hydrogenation method, is highly selective for the reduction of various carbonyl compounds such as furfural (FF), levulinic acid (LA), ethyl levulinate (EL), in which alcohols such as ethanol and isopropanol are commonly employed as hydrogen donors to replace H_2 [52-55]. More satisfyingly, the MPV reaction has been verified to be catalyzed by the inexpensive zirconium-containing catalysts [55-62], which can reduce the corresponding production cost to a large extent. At the same time, HMF with an aldehyde group is also a carbonyl compound; therefore, it should be theoretically applicable to MPV reaction. Inspired by this speculation, a novel catalytic transfer hydrogenation system was developed in this work for the selective transformation of HMF into DHMF via MPV reaction over the zirconium hydroxide catalysts with the introduction of magnetic components. To achieve the ideal catalytic activity, various reaction conditions such as reaction temperature, reaction time, catalyst amount and alcohol type were optimized in detail. Furthermore, the recyclability of catalyst and the plausible reaction mechanism for selective transformation of HMF into DHMF were also investigated.

EXPERIMENTAL

1. Materials

HMF (99%) was supplied by Shanghai Energy Chemical Co. Ltd. (Shanghai, China). DHMF (99%) was purchased from Shanghai Bide Pharmatech Co. Ltd. (Shanghai, China). Zirconium oxychloride octahydrate ($ZrOCl_2{\cdot}8H_2O$) was supplied by Shanghai Aladdin Reagent Co. Ltd. (Shanghai, China). Ferrous sulfate heptahydrate ($FeSO_4{\cdot}7H_2O$), ferric chloride hexahydrate ($FeCl_3{\cdot}6H_2O$), ammonium hydroxide ($NH_3{\cdot}H_2O$), methanol, ethanol, isopropanol, 1-butanol, 2-butanol and many other chemicals were purchased from Sinopharm Chemical Reagent Co. Ltd. (Shanghai, China) and used without further purification.

2. Catalyst Preparation

Magnetic zirconium hydroxides (MZHs) were prepared by a one-pot two-step approach. Primarily, $FeSO_4{\cdot}7H_2O$ (2.78 g, 10 mmol) and $FeCl_3{\cdot}6H_2O$ (5.40 g, 20 mmol) were dissolved in deoxidized and deionized water (DDW, 200 mL) under an atmospheric pressure of nitrogen (N_2) with a agitation speed of 600 rpm. Next, $NH_3{\cdot}H_2O$ was slowly added into the above solution until the value of pH was kept at 10, and the temperature was further elevated to 80 °C. After continuous stirring for 1 h, the reaction mixture was cooled to room temperature, and the black precipitates were collected by a permanent magnet and washed with DDW to neutrality. Subsequently, the resulting precipitates were resuspended in 200 mL DDW and mixed with 400 mL aqueous solution of $ZrOCl_2$ (9.67 g, 30 mmol; 19.34 g, 60 mmol; or 29.01 g, 90 mmol), which was then stirred for 30 min and sonicated for 10 min. Soon afterwards, $NH_3{\cdot}H_2O$ was slowly added into the above mixture until the pH was kept at 10, and the reaction mixture was continually stirred for 30 min and aged for 24 h at room temperature, which was followed by filtrating and washing with DDW until chloride ions were not detected in the washed water. Eventually, the generating magnetic catalysts that were abbreviated as MZH(Zr/Fe=1, 2 or 3) were dried in a vacuum oven at 110 °C for 12 h. For the sake of comparison, other catalysts such as zirconium hydroxide ($Zr(OH)_4$), stannic hydroxide ($Sn(OH)_4$), aluminum hydroxide ($Al(OH)_3$) and ferric hydroxide ($Fe(OH)_3$) were also synthesized by using the similar approach without the introduction of magnetic components.

3. Catalyst Characterization

The patterns of X-ray diffraction (XRD) were recorded on an ARL X'TRA diffractometer (ARL, Switzerland) using a Cu Kα radiation source (λ=0.15418 nm). The images of scanning electron microscopy (SEM) and transmission electron microscopy (TEM) were conducted on a Zeiss Sigma scanning electron microscope (Zeiss, Germany) and a JEM-2100 transmission electron microscope (JEOL, Japan), respectively. The isotherms of nitrogen adsorption-desorption were measured on a 3FLEX surface analyzer (Micromeritics, USA) at −196 °C. Before adsorption, catalysts were degassed at 100 °C for 3 h. The specific surface areas and pore sizes were evaluated using the method of Brunauer-Emmett-Teller (BET) and the method of Barrett-Joyner-Halenda (BJH), respectively. The spectra of Fourier transform infrared (FT-IR) were collected on a Nicolet IS50 spectrometer (Nicolet, USA) using the standard KBr pellet method in the range from 400 cm^{-1} to 4,000 cm^{-1} with a resolution of 4 cm^{-1}. The profiles of ammonia temperature-programmed desorption (NH_3-TPD) and carbon dioxide temperature-programmed desorption (CO_2-TPD) were estimated on an AutoChem II 2920 chemisorption analyzer (CA) (Micromeritics, USA). The magnetic properties were observed on an MPMS-XL-7 superconducting quantum interference device (SQUID) (Quantum, USA) at room temperature in an applied magnetic field of 18,000 Oe. The carbon content was analyzed on a Vario EL III elemental analyzer (EA) (Elementar, Germany).

4. Typical Procedure for the Selective Transformation of HMF into DHMF

All the catalytic transfer hydrogenation reactions were in a 100 mL cylindrical stainless steel reactor (Parr, USA) with the external temperature and stirring controllers. In a typical reaction, the reactor was charged with 0.5 g HMF, 0.3 g catalyst and 24.5 g alcohol, and the reactor was sealed and purged with N_2 for 5 times. And then, the reactor was filled with an atmospheric pressure of N_2 and heated to a known temperature and stirred at a speed of 500 rpm for the specific time. At the end of the reaction, the reactor was immediately quenched to room temperature in an ice-water bath, and the reaction mixture was sampled and filtered with 0.22 μm syringe membrane filter.

5. Product Analysis

HMF, DHMF and other products were analyzed by means of GC (Shimadzu GC-2014) and GC-MS (Shimadzu QP2010) equipped with the flame ionization detector (FID) and the polar capillary column (DB-WAXETR, 30 m×0.32 mm×0.25 μm), respectively. The initial column temperature was 40 °C and maintained for 2 min, and then, the column temperature was increased to 100 °C at a heating rate of 5 °C/min and maintained for 2 min, after that, the column temperature was further increased to 250 °C at a heating rate of 10 °C/min and maintained for 4 min. Moreover, HMF conversion and DHMF yield were quantified via the external standard

method and calculated by using the following equations:

$$\text{HMF conversion (\%)} = \left(1 - \frac{\text{Mole of HMF in products}}{\text{Initial mole of HMF}}\right) \times 100 \quad (1)$$

$$\text{DHMF yield (\%)} = \frac{\text{Mole of DHMF in products}}{\text{Initial mole of HMF}} \times 100 \quad (2)$$

RESULTS AND DISCUSSION

1. Characterization of Catalysts

The preparation process of MZHs can be divided into two consecutive steps in the same reactor: (1) the synthesis of ferroferric oxide (Fe_3O_4) via the method of coprecipitation [63-65]; (2) the encapsulation of zirconium hydroxide ($Zr(OH)_4$) on the surface of Fe_3O_4 [66-68]. Once MZHs are prepared, they will be comprehensively characterized by a sequence of characterization methods such as XRD, TEM, SEM, BET, BJH, FT-IR, NH_3-TPD and CO_2-TPD, and the corresponding characteristic results are summarized in the subsequent section.

Fig. 1 shows the XRD patterns of MZHs and $Zr(OH)_4$. In contrast to $Zr(OH)_4$, the peaks of MZHs at around 30.2°, 35.5°, 43.3°, 53.6°, 57.2° and 62.7° are assigned to (220), (311), (400), (422), (511) and (440) lattice planes of Fe_3O_4, respectively, which is consistent with the standard magnetite structure data in the JCPDS Card No. 19-0629 [69], indicating that Fe_3O_4 components have been successfully introduced into MZHs and their structures are not apparently affected in the encapsulation process of $Zr(OH)_4$ (Fig. S1). Furthermore, note that no other obvious peak is observed

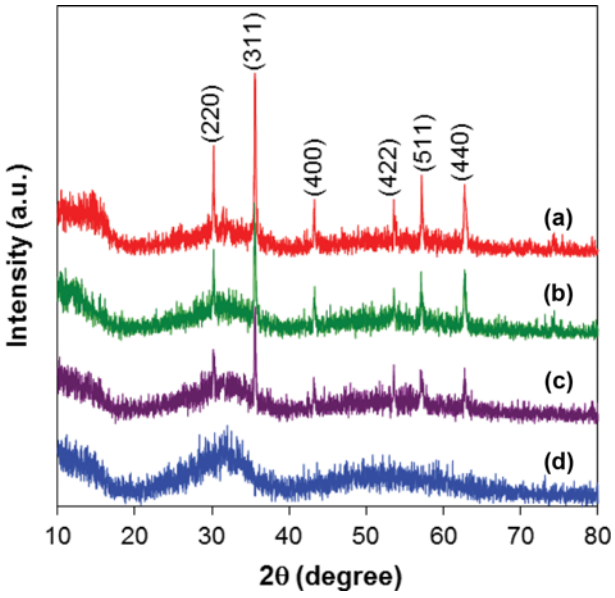

Fig. 1. XRD patterns of (a) MZH(Zr/Fe=1), (b) MZH(Zr/Fe=2), (c) MZH(Zr/Fe=3) and (d) $Zr(OH)_4$.

in Fig. 1, demonstrating that $Zr(OH)_4$ components in MZHs are still presented in the form of amorphous state. From the above results, it can be clearly seen that MZHs not only introduce the magnetic property of Fe_3O_4 but also retain the original state of $Zr(OH)_4$, which is favorable for the catalytic transfer hydrogenation of carbonyl compounds via MPV reaction [57].

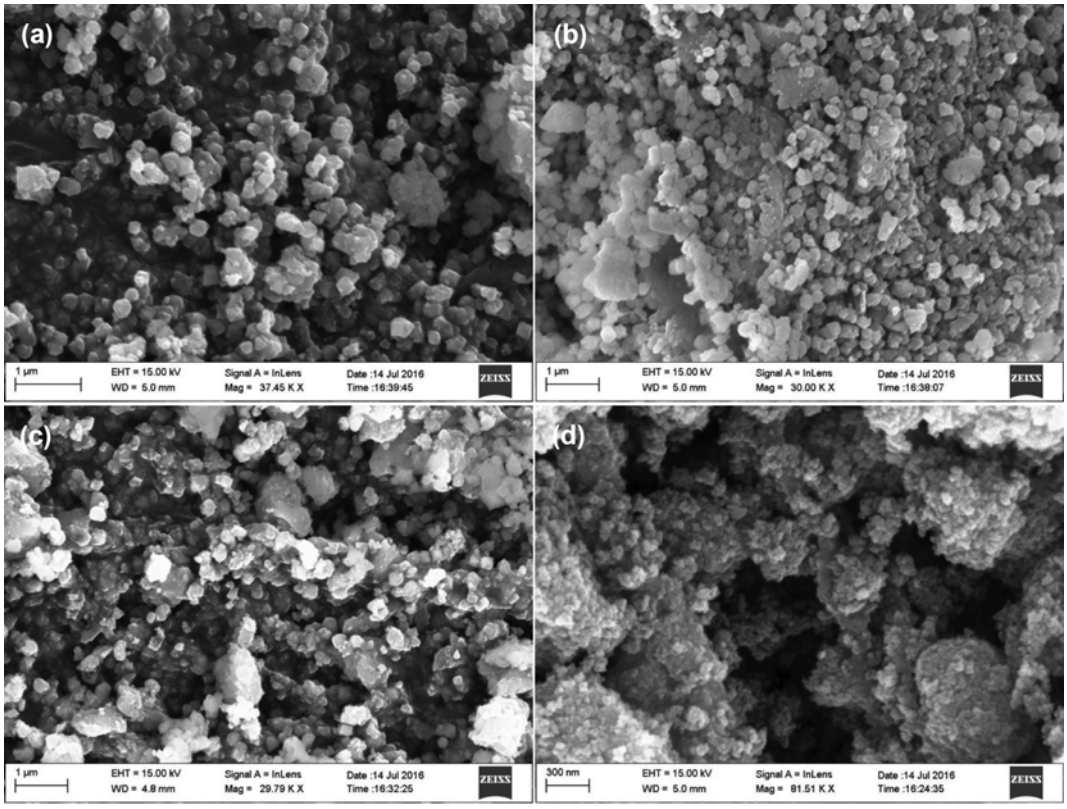

Fig. 2. SEM images of (a) MZH(Zr/Fe=1), (b) MZH(Zr/Fe=2), (c) MZH(Zr/Fe=3) and (d) $Zr(OH)_4$.

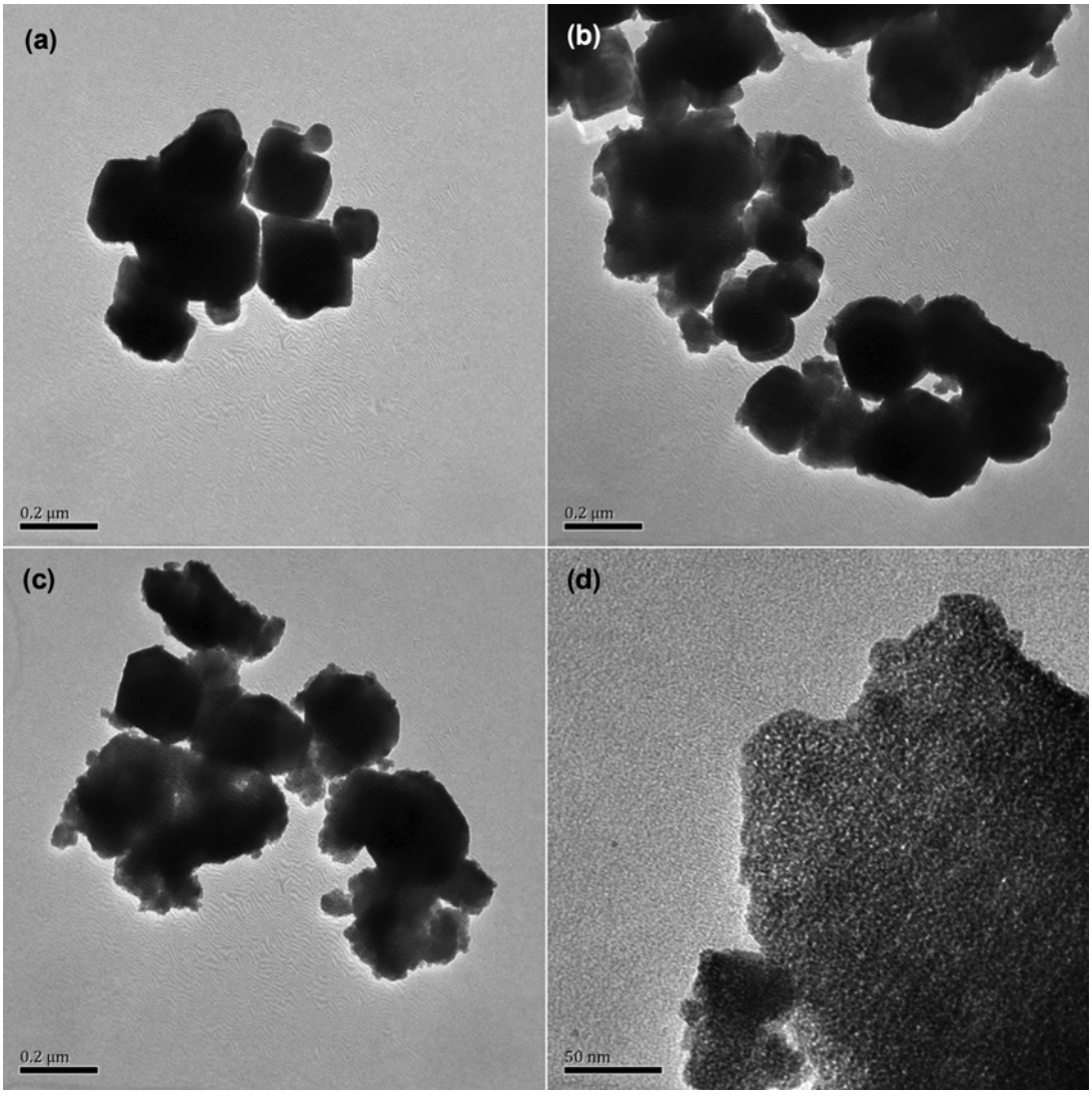

Fig. 3. TEM images of (a) MZH(Zr/Fe=1), (b) MZH(Zr/Fe=2), (c) MZH(Zr/Fe=3) and (d) $Zr(OH)_4$.

Table 1. Selective transformation of HMF into DHMF over various catalysts with different physicochemical properties[a]

Entry	Catalyst	HMF conversion (%)	DHMF yield (%)	Surface area (m^2/g)[b]	Pore size (nm)[c]	Acid content (mmol/g)[d]	Base content (mmol/g)[e]
1	No catalyst	5.7	0	-	-	-	-
2	Fe_3O_4	10.4	1.8	91.8	7.2	1.481	0.264
3	$Al(OH)_3$	26.3	12.9	-	-	-	-
4	$Fe(OH)_3$	31.6	7.4	-	-	-	-
5	$Sn(OH)_4$	41.2	4.4	-	-	-	-
6	$Zr(OH)_4$	71.5	62.7	226.5	2.6	0.287	1.659
7	MZH(Zr/Fe=1)	75.2	66.4	103.4	5.7	1.223	0.785
8	MZH(Zr/Fe=2)	79.9	71.3	165.7	3.1	0.948	1.092
9	MZH(Zr/Fe=3)	82.3	68.9	194.8	2.8	0.752	1.276

[a]Reaction conditions: 0.3 g catalyst, 0.5 g HMF, 24.5 g 2-butanol, 150 °C, 4 h, 1 bar N_2
[b]Surface areas were measured by the method of BET
[c]Pore sizes were measured by the method of BJH
[d]Acid contents were determined by the profile of NH_3-TPD
[e]Base contents were determined by the profile of CO_2-TPD

Fig. 2 and Fig. 3 show the SEM and TEM images of MZHs and $Zr(OH)_4$, respectively. Although all catalysts are aggregated in different degrees, they are composed of primary nanoscale particles. Differently, these primary nanoscale particles in MZHs are relatively bigger and smoother than those in $Zr(OH)_4$, leading to a gradual decrease in the specific surface areas of MZHs (Table 1), which can also be confirmed by the declining adsorption capacities for nitrogen. In addition, according to nitrogen adsorption-desorption isotherms at various relative pressures in Fig. 4, the pore size of $Zr(OH)_4$ is estimated to be smaller than that of MZHs, which should be due to the introduction of Fe_3O_4 facilitating the formation of pores in relatively larger size by restraining the excessive aggregation of primary nanoscale particles in MZHs. Moreover, with the increase of Zr/Fe molar ratios, the specific surface areas and pore sizes of MZHs are correspondingly increased and decreased to a certain extent, respectively, and the specific data is listed in Table 1 and Fig. S2.

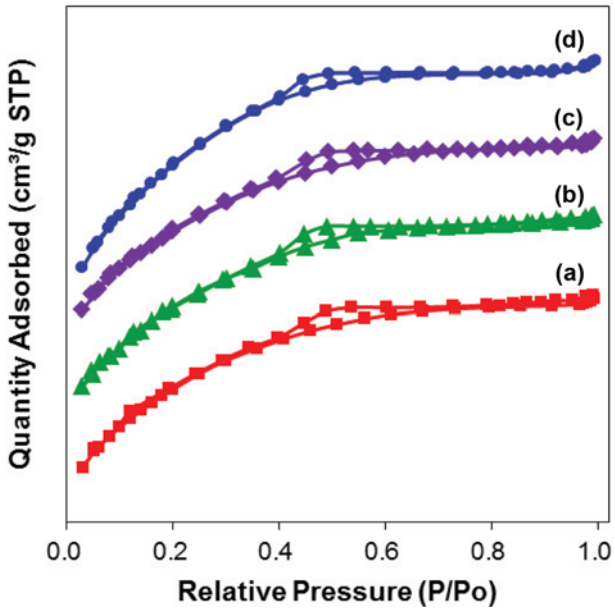

Fig. 4. Nitrogen adsorption-desorption isotherms of (a) MZH(Zr/Fe=1), (b) MZH(Zr/Fe=2), (c) MZH(Zr/Fe=3) and (d) $Zr(OH)_4$.

Fig. 5 shows the FT-IR spectra of MZHs and $Zr(OH)_4$. The peaks at around 3,400 cm^{-1} and 1,626 cm^{-1}, 1,545 cm^{-1}, 1,450 cm^{-1} and 1,334 cm^{-1} are assigned to the stretching and bending vibration of O-H in the hydroxyl groups, respectively, which are related to the basic sites of catalysts that can be able to interact with CO_2 [70-72]. Furthermore, the peak at around 1,090 cm^{-1} is ascribed to the stretching vibration of Zr-O in the zirconyl groups, which are responsible for the acidic sites of catalysts that can be able to interact with NH_3 [72]. In contrast to $Zr(OH)_4$, a new peak in MZHs has emerged at around 586 cm^{-1} that is due to the stretching vibration of Fe-O in the magnetic groups [73-76], which is in agreement with the results of XRD.

Fig. 6 shows the NH_3-TPD profiles of MZHs and $Zr(OH)_4$. In all catalysts, there are two peaks at around 175 °C and 348 °C that are attributed to the weak and medium acidic sites of catalysts, which should be caused by the different interaction modes of zirconium with NH_3 (Fig. S3) [77], respectively. Analogously, as can be seen from the CO_2-TPD profiles of MZHs and $Zr(OH)_4$ in Fig. 7, another two peaks are also observed at around 170 °C and 318 °C, which are ascribed to the weak and medium basic sites of catalysts where CO_2 can be adsorbed in the form of bicarbonate and bidentate carbonate (Fig. S4) [70], respectively. Based on the above results, it is concluded that MZHs and $Zr(OH)_4$ are amphoteric catalysts with the corresponding acid-base properties. Moreover, although the introduction of Fe_3O_4 does not apparently change the acid-base strengths of MZHs, it affects the acid-base contents of MZHs to a large extent. As shown in Table 1, with the increase of Zr/Fe molar ratios, the content of acidic and basic sites in MZHs

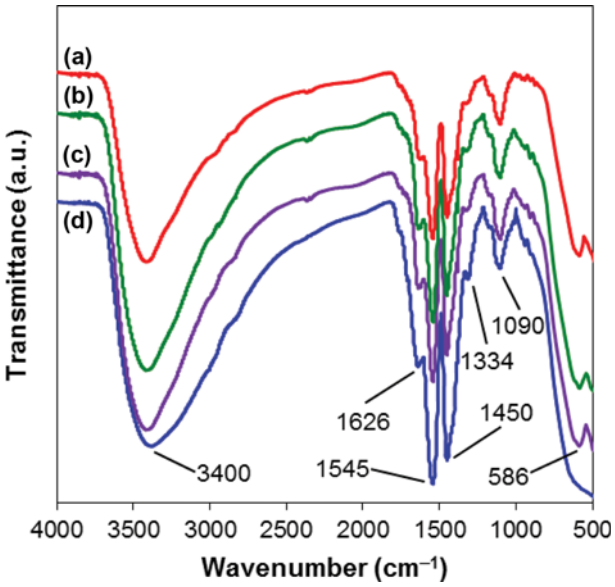

Fig. 5. FT-IR spectra of (a) MZH(Zr/Fe=1), (b) MZH(Zr/Fe=2), (c) MZH(Zr/Fe=3) and (d) $Zr(OH)_4$.

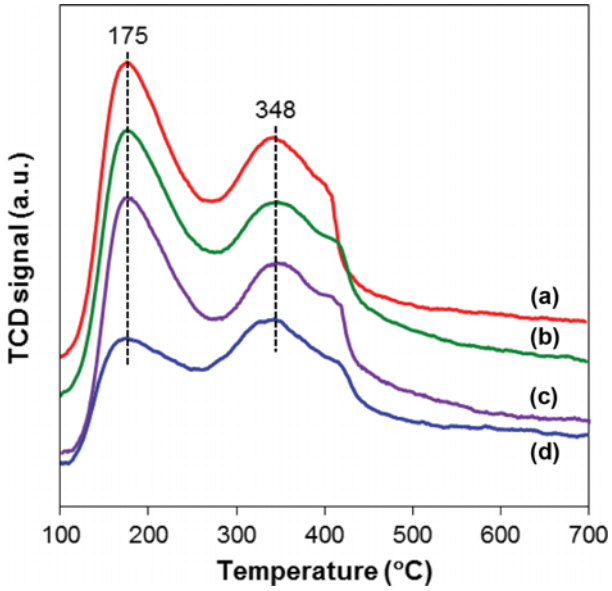

Fig. 6. NH_3-TPD profiles of (a) MZH(Zr/Fe=1), (b) MZH(Zr/Fe=2), (c) MZH(Zr/Fe=3) and (d) $Zr(OH)_4$.

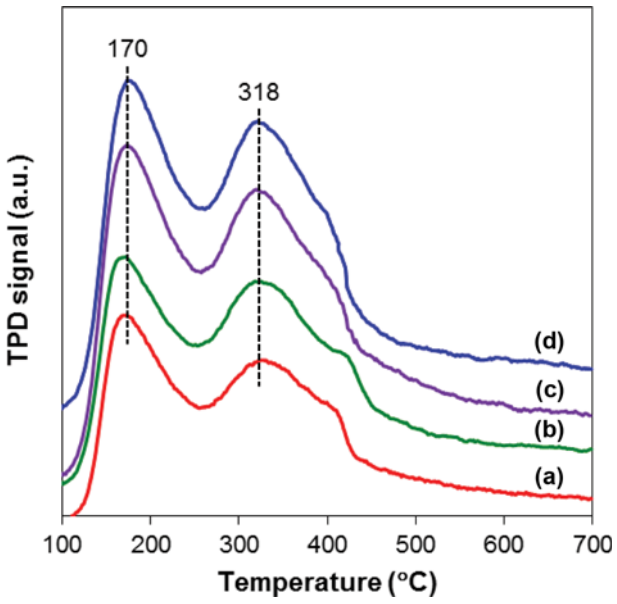

Fig. 7. CO_2-TPD profiles of (a) MZH(Zr/Fe=1), (b) MZH(Zr/Fe=2), (c) MZH(Zr/Fe=3) and (d) $Zr(OH)_4$.

is gradually decreased and increased, respectively.

2. Preliminary Study on Different Catalyst Types for the Selective Transformation of HMF into DHMF

To the best of our knowledge, the selective transformation of HMF into DHMF via the method of catalytic transfer hydrogenation over the inexpensive zirconium-containing magnetic catalysts has not been reported in the previous studies. Hence, in order to verify the feasibility of this new system, the catalytic activities of MZHs, $Zr(OH)_4$ and other catalysts were first evaluated in the presence of 2-butanol that could be acting as hydrogen donor as well as reaction medium. As can be seen from Table 1, HMF conversion and DHMF yield largely relied on the applied catalysts. In the absence of any catalyst, although 5.7% HMF was converted at 150 °C for 4 h, the yield of DHMF was negligible, which obviously indicates that the usage of catalysts was very essential for the successful transformation of HMF into DHMF. Under the same reaction conditions, when Fe_3O_4 was used as a catalyst, HMF conversion and DHMF yield were only 10.4% and 1.8%, respectively, demonstrating that it was almost inactive for the selective transformation of HMF into DHMF. When the catalysts were changed into $Al(OH)_3$, $Fe(OH)_3$ and $Sn(OH)_4$, 12.9%, 7.4% and 4.4% yields of DHMF could be obtained, respectively, however, the conversion of HMF was always lower than 42.0%. Surprisingly, if $Zr(OH)_4$ was applied for the selective transformation of HMF into DHMF, HMF conversion and DHMF yield were sharply improved to 71.5% and 62.7%, respectively, which should be due to its larger specific surface area and higher base content [56].

With regard to the above phenomena, the specific surface areas and basic sites of catalysts have been proved to be very important for the catalytic transfer hydrogenation of carbonyl compounds via MPV reaction in many studies [56-58]; however, they are not the only two factors in this study, which can be further verified by entries 7, 8 and 9 in Table 1. Compared with $Zr(OH)_4$, although MZHs with the introduction of Fe_3O_4 contained the smaller specific surface areas and lower base contents, they still led to more than 75.0% HMF conversion and 65.0% DHMF yield, clearly demonstrating that the pore sizes and acidic sites of catalysts were also crucial for the selective transformation of HMF into DHMF. Thus, it can be concluded that the synergistic effects of acidic sites, basic sites, specific surface areas and pore sizes should be answerable to the superior catalytic activities of MZHs, in which the higher acid content and base content could promote the activation of carbonyl group of HMF and the dissociation of hydroxyl group of 2-butanol [52], and the larger specific surface areas and pore sizes could enhance the contact of HMF and MZHs and facilitate the synthesis of DHMF with the less formation of byproducts [68], respectively. In addition, among three magnetic catalysts, MZH(Zr/Fe=2) with the moderate specific surface area, pore size and acid-base content exhibited the highest catalytic activity, resulting in 79.9% HMF conversion and 71.3% DHMF yield. Therefore, MZH(Zr/Fe=2) was selected as the appropriate catalyst for the following experiments.

3. Intensive Study on Various Reaction Conditions for the Selective Transformation of HMF into DHMF over MZH(Zr/Fe=2)

It is common knowledge that the catalytic activities of catalysts are also strongly dependent on various reaction conditions in addition to catalyst properties. Hence, to better understand their effects on the selective transformation of HMF into DHMF over the catalyst of MZH(Zr/Fe=2), reaction temperature, reaction time, catalyst amount and alcohol type were investigated in detail. Moreover, the recyclability of MZH(Zr/Fe=2) was also studied in this section.

As presented in Fig. 8, only 38.4% HMF conversion and 33.2% DHMF yield were obtained at a lower reaction temperature of 130 °C. With the increase of reaction temperature to 150 °C, HMF conversion and DHMF yield were dramatically increased to 79.9% and 71.3%, respectively, which reveals that the selective transfor-

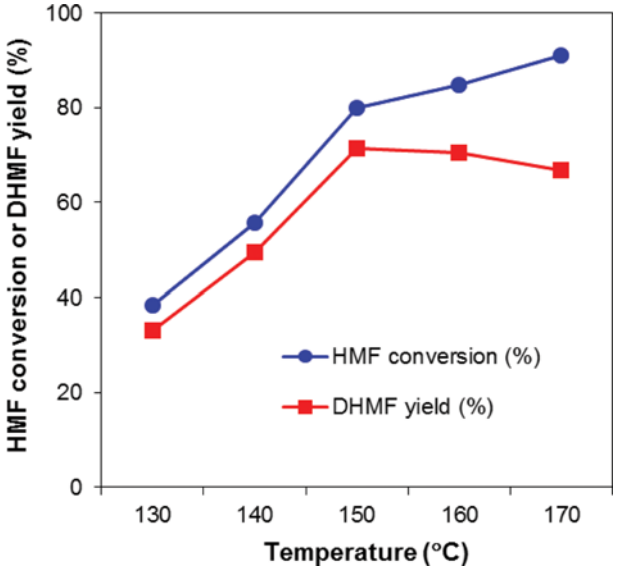

Fig. 8. Effect of reaction temperature on the selective transformation of HMF into DHMF. Reaction conditions: 0.3 g MZH(Zr/Fe=2), 0.5 g HMF, 24.5 g 2-butanol, 4 h, 1 bar N_2.

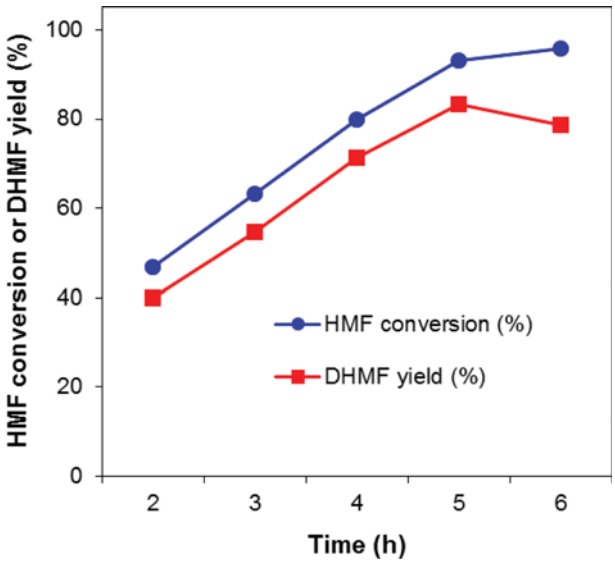

Fig. 9. Effect of reaction time on the selective transformation of HMF into DHMF. Reaction conditions: 0.3 g MZH(Zr/Fe=2), 0.5 g HMF, 24.5 g 2-butanol, 150 °C, 1 bar N_2.

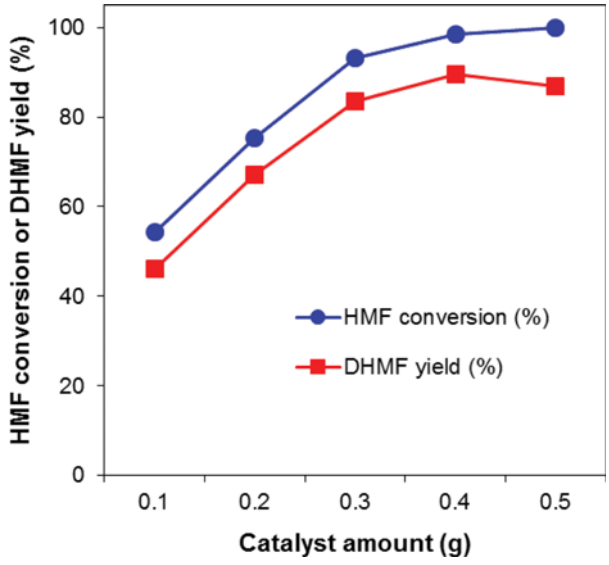

Fig. 10. Effect of MZH(Zr/Fe=2) amount on the selective transformation of HMF into DHMF. Reaction conditions: 0.5 g HMF, 24.5 g 2-butanol, 150 °C, 5 h, 1 bar N_2.

mation of HMF into DHMF could be promoted by a higher reaction temperature. Furthermore, when the reaction temperature was further increased to 170 °C, although the conversion of HMF was up to 91.1%, the yield of DHMF was decreased to 66.8%, which should be ascribed to the fact that too much higher temperature gave rise to a series of side-reactions such as the hydrogenolysis of HMF and DHMF into 5-methylfurfural (MF) and 5-methylfurfuryl alcohol (MFA) [8] that could be detected by GC-MS (Fig. S5 and Fig. S6). According to these results, the proper reaction temperature was set to 150 °C.

As indicated in Fig. 9, when the reaction time was 2 h, HMF conversion and DHMF yield were merely 46.8% and 39.9%, respectively. With the extension of reaction time from 3 h to 5 h, the conversion of HMF and the yield of DHMF were significantly increased from 63.2% and 54.6% to 93.1% and 83.4%, respectively. When the reaction time was further prolonged to 6 h, although most of HMF with 95.9% was converted, DHMF yield was not continuously increased but decreased to 78.6%. In general, DHMF yield is manipulated by a balance in the hydrogenation and hydrogenolysis of HMF (Fig. S7). At the beginning of the reaction, the hydrogenation rate of HMF was much greater than the hydrogenolysis rate of HM; thus, the yield of DHMF was gradually increased with the increase of reaction time. When the hydrogenolysis rate of HMF was equal to the hydrogenation rate of HMF, the yield of DHMF reached to a peak value. After that, the hydrogenolysis rate of HMF would be greater than the hydrogenation rate of HMF, the yield of DHMF began to decrease, which is in accordance with the trend of Fig. 9. Hence, it is considered that a reaction time of 5 h was suitable at the reaction temperature of 150 °C.

As illustrated in Fig. 10, when the amount of MZH(Zr/Fe=2) was increased from 0.1 g to 0.4 g, HMF conversion and DHMF yield were successively increased from 54.4% and 46.1% to 99.9% and 89.6%, respectively, demonstrating that increasing the amount of MZH(Zr/Fe=2) in a certain scope could not only promote the conversion of HMF but also facilitate the formation of DHMF. However, when the amount of MZH(Zr/Fe=2) was further increased to 0.5 g, the yield of DHMF was decreased to 86.8% although 99.9% conversion of HMF was achieved, which should have been caused by much more available active sites derived from the excessive MZH(Zr/Fe=2) that accelerated the occurrence of various byproducts such as MF and MFA. Furthermore, the overuse of MZH(Zr/Fe=2) could also increase the production cost of DHMF to a large extent. Thus, considering the satisfactory yield and production cost of DHMF, 0.4 g MZH(Zr/Fe=2) was preferred at 150 °C for 5 h.

As listed in Table 2, HMF conversion and DHMF yield are highly associated with the reduction potentials (ΔH_f^o) of alcohols that decrease in the order of methanol>ethanol>1-butanol>isopropanol≈2-butanol [78]. It is generally known that the reduction potentials are defined as the difference of the standard molar enthalpy of for-

Table 2. Effect of alcohol type on the selective transformation of HMF into DHMF[a]

Alcohol	HMF conversion (%)	DHMF yield (%)	ΔH_f^o (kJ/mol)
Methanol	66.2	3.3	130.1[b]
Ethanol	90.3	82.5	85.4[b]
Isopropanol	97.1	88.7	70.0[c]
1-Butanol	84.7	76.4	79.7[c]
2-Butanol	98.4	89.6	69.3[c]

[a]Reaction conditions: 0.4 g MZH(Zr/Fe=2), 0.5 g HMF, 24.5 g 2-butanol, 150 °C, 5 h, 1 bar N_2

[b]The numerical values of ΔH_f^o were calculated according to the definition of ΔH_f^o

[c]The numerical values of ΔH_f^o were obtained from the previous report [78]

mation between alcohols and their corresponding carbonyl products, and that is to say, they represent the complexity of hydrogen abstraction [79]. Because methanol possesses the highest reduction potential in various alcohols, therefore, although the selective transformation of HMF into DHMF was carried out under the optimum reaction conditions, it still showed a poor capacity as hydrogen donor. However, on this occasion, 5-hydroxymethyl-2-(dimethoxymethyl)furan (HMDMMF) was identified as the dominant byproduct (Fig. S8), which was formed by the acetalization of HMF with methanol. When ethanol was used as hydrogen donor, the conversion of HMF and the yield of DHMF were 90.3% and 82.5%, respectively; they were more than those in 1-butanol, and even the reduction potential of 1-butanol is lower than that of ethanol, which may be due to the stronger steric effect of 1-butanol [56]. Expectedly, compared with the above primary alcohols, the secondary alcohols such as isopropanol and 2-butanol with much lower reduction potentials were more active for the selective transformation of HMF into DHMF, resulting in more than 97.0% HMF conversion and 88.0% DHMF yield. In particular, the best results were observed in the presence of 2-butanol; hence, it was chosen as the outstanding hydrogen donor in this work. Moreover, MZH (Zr/Fe=2) and 2-butanol is an excellent combination for the selective hydrogenation of HMF; the obtained yield of DHMF can be comparable to that in the previous studies (Table 3).

The recyclability of catalyst is extremely important to appraise the stability of catalyst, which is beneficial to reduce the cost of practical production in the selective transformation of HMF into DHMF. In the recycling experiments, when each reaction run was accomplished, the catalyst of MZH(Zr/Fe=2) with a superior magnetic property would be separated from the reaction mixture by an outer magnet (Fig. 11). After separation, MZH(Zr/Fe=2) was repeatedly washed with DDW and ethanol, and then dried in a vacuum oven at 110 °C for 12 h. Subsequently, the recovered MZH (Zr/Fe=2) was directly reused in the next reaction run under the same reaction conditions. As depicted in Fig. 12, no apparent decrease in the catalytic activity of MZH(Zr/Fe=2) was observed after three successive reaction runs, and the conversion of HMF and the yield of DHMF were still achieved to 95.2% and 87.3%, respectively, indicating that MZH(Zr/Fe=2) showed good catalytic stability. Moreover, HMF conversion and DHMF yield were decreased to 89.7% and 80.2% in the fourth reaction run, respectively. Because the pore size and acid-base content of MZH(Zr/Fe=2) did not remarkably change (Table S1), this unacceptable decrease in the catalytic activity of MZH(Zr/Fe=2) was possibly due to the decrease of specific surface area of MZH(Zr/Fe=2) that

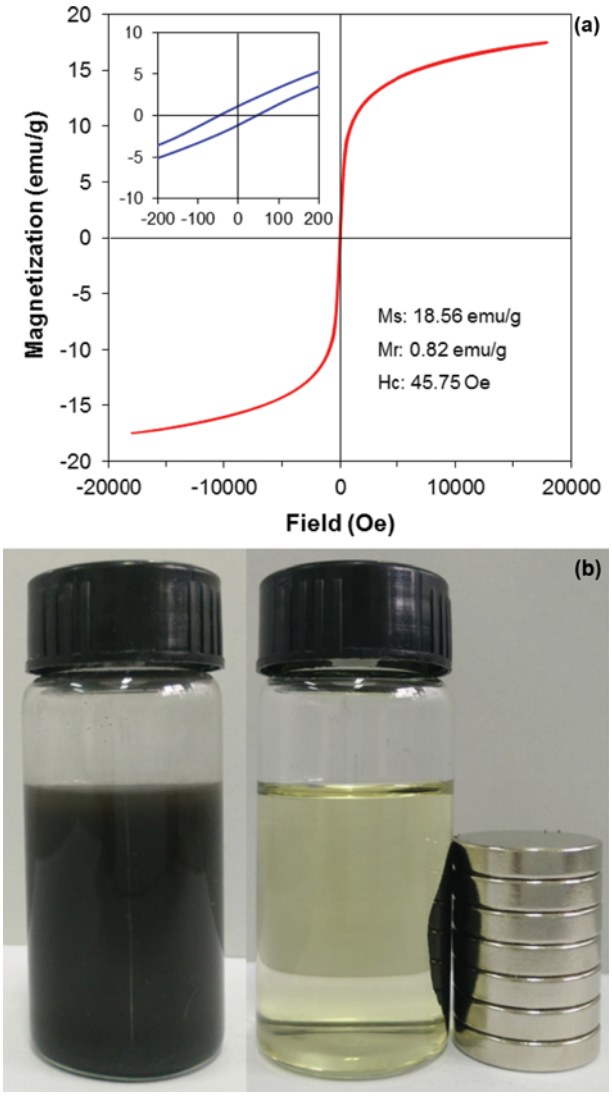

Fig. 11. Magnetic curve (a) and separation (b) of MZH(Zr/Fe=2).

Table 3. Comparison of various catalytic systems for the selective transformation of HMF into DHMF

Entry	Hydrogen donor	Pressure (bar)	Catalyst, amount (wt%)[a]	Temperature (°C), time (h)	HMF conversion (%)	DHMF yield (%)	Reference
1	H_2	27	Ru/Al_2O_3, 17	130, 2	92.0	81.0	[36]
2	H_2	100	Pt/C, 5	80, 20	97.0	82.0	[38]
3	H_2	30	Au/FeO_x, 40	80, 2	96.0	96.0	[40]
4	H_2	60	Ir/TiO_2, 53	50, 3	99.0	94.1	[42]
5	HMF	-	NaOH, 35	0, 36	-	82.0	[46]
6	Ethanol	-	$ZrO(OH)_2$, 100	150, 5/2	94.1	83.7	[11]
7	Isopropanol	-	Zr-FDCA-T, 40	140, 8	97.0	87.0	[62]
8	2-Butanol	-	MZH(Zr/Fe=2), 80	150, 5	98.4	89.6	This work

[a]The amount of catalyst is based on the amount of HMF

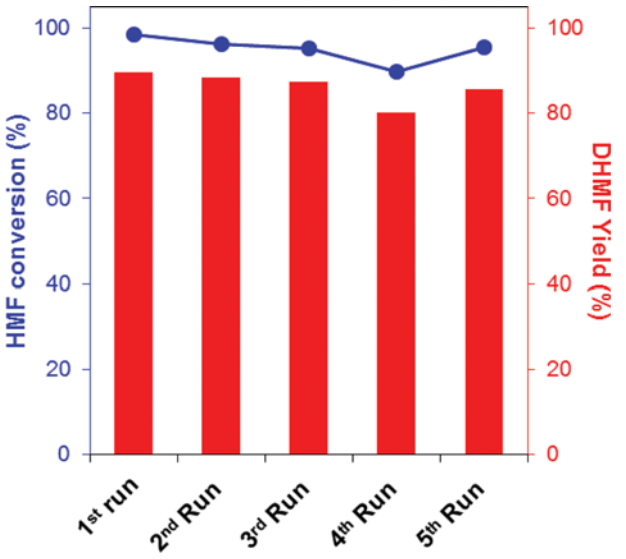

Fig. 12. Recycling of MZH(Zr/Fe=2). Reaction conditions: 0.4 g MZH (Zr/Fe=2), 0.5 g HMF, 24.5 g 2-butanol, 150 °C, 5 h, 1 bar N_2.

Table 4. Carbon content and surface area of MZH(Zr/Fe=2) in the recycling process

Recycle run	Carbon content (%)[a]	Surface area (m^2/g)[b]
Fresh	0	165.7
4	7.3	139.6
Regenerated	1.4	158.2

[a]Carbon contents were determined by EA
[b]Surface areas were measured by the method of BET

which can be further confirmed by the elemental analysis of MZH (Zr/Fe=2) in Table 4. Fortunately, the partial deactivation of MZH (Zr/Fe=2) could be readily regenerated by a simple calcination at 300 °C for 5 h, and when the regenerated MZH(Zr/Fe=2) was reused in the fifth reaction run, comparable results with 95.6% HMF conversion and 85.8% DHMF yield were obtained in Fig. 12.

4. Exploratory Study on Reaction Mechanism for the Selective Transformation of HMF into DHMF over MZH(Zr/Fe=2) in 2-Butanol

From the above results, it can be seen that MZH(Zr/Fe=2) displayed the preeminent catalytic activity and stability for the selective transformation of HMF into DHMF via the method of catalytic transfer hydrogenation in the presence of 2-butanol. To gain more insight into the authentic reaction mechanism, some auxiliary experiments were also conducted by introducing various additives into the reactor. As shown in Table 5, the higher pressure of N_2 with 5 bar at the beginning of reaction was found to be negative for the catalytic transfer hydrogenation of HMF into DHMF; therefore, an atmospheric pressure of N_2 with 1 bar was adopted in this work. According to previous reports [80-82], hydride transfer is believed to be responsible for the catalytic transfer hydrogenation of HMF into DHMF via MPV reduction. Although the direct evidences have not been observed to imply the existence of hydrides, they can be indirectly proved by the variation of water content in the

Table 5. Selective transformation of HMF into DHMF over MZH (Zr/Fe=2) in 2-butanol with the addition of various additives[a]

Additive	HMF conversion (%)	DHMF yield (%)	Water content (%)[c]
1 bar N_2	98.4	89.6	1.07
5 bar N_2	95.8	83.7	-
1 bar O_2	84.5	65.4	1.69
5 bar O_2	71.3	37.8	2.78
Pyridine[b]	88.9	79.3	-
Benzoic acid[b]	39.7	24.5	-

[a]Reaction conditions: 0.4 g MZH(Zr/Fe=2), 0.5 g HMF, 24.5 g 2-butanol, 150 °C, 5 h
[b]0.2 g additive and 1 bar N_2 were added into the reactor
[c]The content of water in the reaction mixture was measured by a V20 moisture analyzer (Mettler, Switzerland)

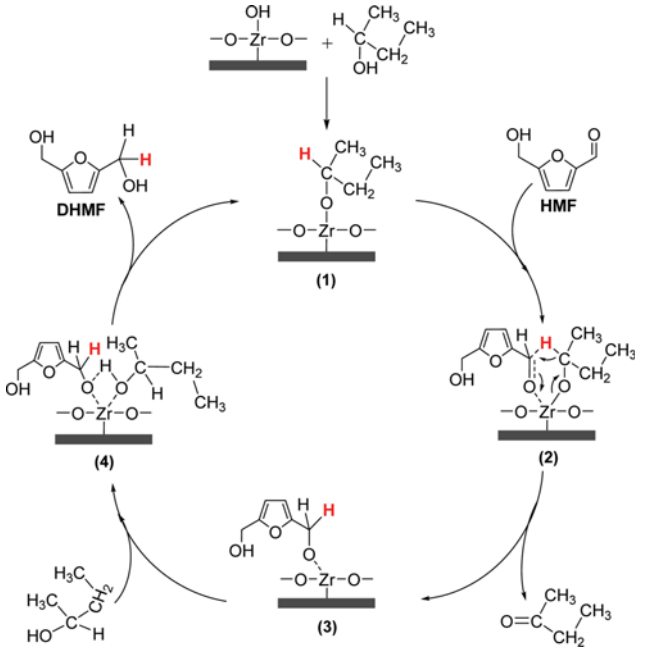

Scheme 1. Plausible reaction mechanism for the catalytic transfer hydrogenation of HMF into DHMF over MZH(Zr/Fe=2) in 2-butanol.

reaction mixture. When the reactor was filled with 1 bar and 5 bar O_2 at the beginning of reaction, water content was 1.69% and 2.78% which was much higher than that in the absence of O_2, respectively, which demonstrates that O_2 could compete with HMF to capture the hydrides, leading to an obvious decrease in HMF conversion and DHMF yield. Furthermore, when benzoic acid and pyridine were added into the reactor, the conversion of HMF and the yield of DHMF decreased in different degrees, respectively. However, the inactive tendency of MZH(Zr/Fe=2) was worse in the presence of benzoic acid than pyridine, which indicates that MZH(Zr/Fe=2) was more sensitive to benzoic acid than pyridine, and its catalytic activity was closely related to the basic sites. In other words, although the synergistic effects reliably existed in the

acidic sites and basic sites of MZH(Zr/Fe=2), hydroxyl groups as the basic sites seemingly played a more important role in the catalytic transfer hydrogenation of HMF into DHMF.

Based on these observations and discussions combined with the results of catalyst characterizations and relevant studies [80-82], a plausible reaction mechanism for the catalytic transfer hydrogenation of HMF into DHMF over MHZ(Zr/Fe=2) in 2-butanol was proposed in Scheme 1. To be specific, 2-butanol was first adsorbed on the surface of MZH(Zr/Fe=2) and then dissociated to the corresponding zirconium alkoxide **(1)** via the concerted interaction between the hydroxyl group of alcohol and the hydroxyl group of catalyst. Subsequently, the carbonyl group of HMF was activated by the zirconium metal center of **(1)** to generate the transition state **(2)**. Soon after, the hydride was transferred from the dissociated alcohol to the activated carbonyl carbon via a six-membered ring structure, and at this process, a new carbonyl compound was released to form the intermediate **(3)**. Eventually, another molecule of 2-butanol was coordinated with **(3)** to produce DHMF via the intermediate **(4)**, in which **(1)** would be regenerated and entered into the next catalytic recycle.

CONCLUSIONS

The selective transformation of HMF into DHMF via the method of catalytic transfer hydrogenation in the presence of 2-butanol over the inexpensive magnetic catalyst of MHZ(Zr/Fe=2) was first accomplished in this work, leading to a good yield of DHMF with 89.6% in 5 h at a moderate reaction temperature of 150 °C. This satisfactory result is attributed to the appropriate specific surface area, pore size and acid-base content of MHZ(Zr/Fe=2) as well as the lower reduction potential of 2-butanol. Furthermore, the exploratory study indicated that the basic hydroxyl groups with the aid of acidic zirconium metal centers were affirmed to be very important for the pivotal hydride transfer via a six-membered ring structure in the catalytic transfer hydrogenation of HMF into DHMF over MHZ(Zr/Fe=2) in 2-butanol. In addition, we believe that the combination of MHZ(Zr/Fe=2) and 2-butanol in this work should also be applicable to the catalytic transfer hydrogenation of other biomass-derived molecules such as FF, LA and EL.

ACKNOWLEDGEMENTS

This work was financially supported by the National Natural Science Foundation of China (21506071), the Natural Science Foundation of Jiangsu Province (BK20150413), the Natural Science Foundation of the Higher Education Institutions of Jiangsu Province (16KJA530001), the Key Research and Development Plan of Huaian City (HAS201601-1) and the Special Foundation of Jiangsu Collaborative Innovation Center of Regional Modern Agriculture & Environmental Protection (HSXT229 and HSXT310).

SUPPORTING INFORMATION

Additional information as noted in the text. This information is available via the Internet at http://www.springer.com/chemistry/journal/11814.

REFERENCES

1. M. Besson, P. Gallezot and C. Pinel, *Chem. Rev.*, **114**, 1827 (2014).
2. S. Ummartyotin and H. Manuspiya, *Renew. Sustain. Energy Rev.*, **41**, 402 (2015).
3. L. Hu, L. Lin, Z. Wu, S. Y. Zhou and S. J. Liu, *Appl. Catal. B: Environ.*, **174-175**, 225 (2015).
4. H. Kobayashi, H. Kaiki, A. Shrotri, K. Techikawara and A. Fukuoka, *Chem. Sci.*, **7**, 692 (2016).
5. F. Rosillo-Calle, *J. Chem. Technol. Biotechnol.*, **91**, 1933 (2016).
6. L. Hu, X. Tang, Z. Wu, L. Lin, J. X. Xu, N. Xu and B. L. Dai, *Chem. Eng. J.*, **263**, 299 (2015).
7. M. Moreno-Recio, J. Santamaría-González and P. Maireles-Torres, *Chem. Eng. J.*, **303**, 22 (2016).
8. J. Jae, W. Zheng, R. F. Lobo and D. G. Vlachos, *ChemSusChem*, **6**, 1158 (2013).
9. N. Jiang, W. Qi, R. L. Huang, M. F. Wang, R. X. Su and Z. M. He, *J. Chem. Technol. Biotechnol.*, **89**, 56 (2014).
10. M. Zuo, K. Le, Z. Li, Y. T. Jiang, X. H. Zeng, X. Tang, Y. Sun and L. Lin, *Ind. Crops Prod.*, **99**, 1 (2017).
11. W. W. Hao, W. F. Li, X. Tang, X. H. Zeng, Y. Sun, S. J. Liu and L. Lin, *Green Chem.*, **18**, 1080 (2016).
12. Z. J. Wei, J. T. Lou, Z. B. Li and Y. X. Liu, *Catal. Sci. Technol.*, **6**, 6217 (2016).
13. N. Perret, A. Grigoropoulos, M. Zanella, T. D. Manning, J. B. Claridge and M. J. Rosseinsky, *ChemSusChem*, **9**, 521 (2016).
14. S. X. Yao, X. C. Wang, Y. J. Jiang, F. Wu, X. G. Chen and X. D. Mu, *ACS Sustain. Chem. Eng.*, **2**, 173 (2013).
15. F. Wang, Z. L. Yuan, B. Liu, S. H. Chen and Z. H. Zhang, *J. Ind. Eng. Chem.*, **38**, 181 (2016).
16. L. C. Gao, K. J. Deng, J. D. Zheng, B. Liu and Z. H. Zhang, *Chem. Eng. J.*, **270**, 444 (2015).
17. A. Q. Liu, Z. H. Zhang, Z. F. Fang, B. Liu and K. C. Huang, *J. Ind. Eng. Chem.*, **20**, 1977 (2014).
18. G. Chieffi, M. Braun and D. Esposito, *ChemSusChem*, **8**, 3590 (2015).
19. Z. W. Xu, P. F. Yan, H. X. Li, K. R. Liu, X. M. Liu, S. Y. Jia and Z. C. Zhang, *ACS Catal.*, **6**, 3784 (2016).
20. D. J. Liu, Y. T. Zhang and E. Y. X. Chen, *Green Chem.*, **14**, 2738 (2012).
21. K. Mliki and M. Trabelsi, *Ind. Crops Prod.*, **78**, 91 (2015).
22. F. M. Geilen, T. vom Stein, B. Engendahl, S. Winterle, M. A. Liauw, J. Klankermayer and W. Leitner, *Angew. Chem. Int. Ed.*, **50**, 6831 (2011).
23. C. Moreau, M. N. Belgacem and A. Gandini, *Top. Catal.*, **27**, 11 (2014).
24. A. Gelmini, S. Albonetti, F. Cavani, C. Cesari, A. Lolli, V. Zanotti and R. Mazzoni, *Appl. Catal. B: Environ.*, **180**, 38 (2016).
25. Y. Nakagawa, M. Tamura and K. Tomishige, *ACS Catal.*, **3**, 2655 (2013).
26. Y. Kwon, E. de Jong, S. Raoufmoghaddam and M. T. Koper, *ChemSusChem*, **6**, 1659 (2013).
27. Y. Jiang, A. J. Woortman, G. O. Alberda van Ekenstein, D. M. Petrovic and K. Loos, *Biomacromolecules*, **15**, 2482 (2014).
28. N. R. Jang, H. R. Kim, C. T. Hou and B. S. Kim, *Polym. Adv. Technol.*, **24**, 814 (2013).

29. A. Gandini, *Green Chem.*, **13**, 1061 (2011).
30. Q. Cao, W. Y. Liang, J. Guan, L. Wang, Q. Qu, X. Z. Zhang, X. C. Wang and X. D. Mu, *Appl. Catal. A: Gen.*, **481**, 49 (2014).
31. M. Balakrishnan, E. R. Sacia and A. T. Bell, *Green Chem.*, **14**, 1626 (2012).
32. J. M. Timko and D. J. Cram, *J. Am. Chem. Soc.*, **96**, 7159 (1974).
33. L. Hu, L. Lin and S. J. Liu, *Ind. Eng. Chem. Res.*, **53**, 9969 (2014).
34. B. Op De Beeck, M. Dusselier, J. Geboers, J. Holsbeek, E. Morré, S. Oswald, L. Giebeler and B. F. Sels, *Energy Environ. Sci.*, **8**, 230 (2015).
35. J. S. Han, Y. H. Kim, H. S. Jang, S. Y. Hwang, J. Jegal, J. W. Kim and Y. S. Lee, *RSC Adv.*, **6**, 93394 (2016).
36. R. Alamillo, M. Tucker, M. Chia, Y. Pagán-Torres and J. Dumesic, *Green Chem.*, **14**, 1413 (2012).
37. J. Z. Chen, F. Lu, J. J. Zhang, W. Q. Yu, F. Wang, J. Gao and J. Xu, *ChemCatChem*, **5**, 2822 (2013).
38. F. Liu, M. Audemar, K. De Oliveira Vigier, J.-M. Clacens, F. De Campo and F. Jérôme, *Green Chem.*, **16**, 4110 (2014).
39. M. Chatterjee, T. Ishizaka and H. Kawanami, *Green Chem.*, **16**, 4734 (2014).
40. J. Ohyama, Y. Hayashi, K. Ueda, Y. Yamamoto, S. Arai and A. Satsuma, *J. Phys. Chem. C*, **120**, 15129 (2016).
41. J. Ohyama, A. Esaki, Y. Yamamoto, S. Arai and A. Satsuma, *RSC Adv.*, **3**, 1033 (2013).
42. H. L. Cai, C. Z. Li, A. Q. Wang and T. Zhang, *Catal. Today*, **234**, 59 (2014).
43. M. Tamura, K. Tokonami, Y. Nakagawa and K. Tomishige, *Chem. Commun.*, **49**, 7034 (2013).
44. E. S. Kang, D. W. Chae, B. Kim and Y. G. Kim, *J. Ind. Eng. Chem.*, **18**, 174 (2012).
45. G. Li, Z. Sun, Y. E. Yan, Y. H. Zhang and Y. Tang, *ChemSusChem*, **10**, 494 (2017).
46. S. Subbiah, S. P. Simeonov, J. M. S. S. Esperança, L. P. N. Rebelo and C. A. M. Afonso, *Green Chem.*, **15**, 2849 (2013).
47. Y. Kwon, Y. Y. Birdja, S. Raoufmoghaddam and M. T. Koper, *ChemSusChem*, **8**, 1745 (2015).
48. J. J. Roylance, T. W. Kim and K.-S. Choi, *ACS Catal.*, **6**, 1840 (2016).
49. Y. Kwon, K. J. P. Schouten, J. C. van der Waal, E. De Jong and M. T. M. Koper, *ACS Catal.*, **6**, 6704 (2016).
50. Y. Y. Guo and J. Z. Chen, *RSC Adv.*, **6**, 101968 (2016).
51. Y. M. Li, X. Y. Zhang, N. Li, P. Xu, W. Y. Lou and M. H. Zong, *ChemSusChem*, **10**, 372 (2017).
52. M. J. Gilkey and B. J. Xu, *ACS Catal.*, **6**, 1420 (2016).
53. D. Scholz, C. Aellig and I. Hermans, *ChemSusChem*, **7**, 268 (2013).
54. H. Li, Z. Fang, J. He and S. Yang, *ChemSusChem*, **10**, 681 (2017).
55. J. L. Song, B. W. Zhou, H. c. Zhou, L. Q. Wu, Q. L. Meng, Z. M. Liu and B. X. Han, *Angew. Chem. Int. Ed.*, **54**, 9399 (2015).
56. X. Tang, H. W. Chen, L. Hu, W. W. Hao, Y. Sun, X. H. Zeng, L. Lin and S. J. Liu, *Appl. Catal. B: Environ.*, **147**, 827 (2014).
57. X. Tang, L. Hu, Y. Sun, G. Zhao, W. W. Hao and L. Lin, *RSC Adv.*, **3**, 10277 (2013).
58. X. Tang, X. H. Zeng, Z. Li, W. F. Li, Y. T. Jiang, L. Hu, S. J. Liu, Y. Sun and L. Lin, *ChemCatChem*, **7**, 1372 (2015).
59. J. He, H. Li, Y. M. Lu, Y. X. Liu, Z. B. Wu, D. Y. Hu and S. Yang, *Appl. Catal. A: Gen.*, **510**, 11 (2016).
60. A. Osatiashtiani, A. F. Lee and K. Wilson, *J. Chem. Technol. Biotechnol.*, **92**, 1125 (2017).
61. Z. M. Xue, J. Y. Jiang, G. F. Li, W. C. Zhao, J. F. Wang and T. C. Mu, *Catal. Sci. Technol.*, **6**, 5374 (2016).
62. H. Li, X. F. Liu, T. T. Yang, W. F. Zhao, S. Saravanamurugan and S. Yang, *ChemSusChem*, **18**, 1761 (2017).
63. Z. Zheng, J. L. Wang, H. L. Chen, L. B. Feng, R. Jing, M. Z. Lu, B. Hu and J. B. Ji, *ChemCatChem*, **6**, 1626 (2014).
64. M. S. Luo, S. H. Yuan, M. Tong, P. Liao, W. J. Xie and X. F. Xu, *Water Res.*, **48**, 190 (2014).
65. L. B. Feng, J. L. Wang, L. Chen, M. Z. Lu, Z. Zheng, R. Jing, H. L. Chen and X. B. Shen, *ChemCatChem*, **7**, 616 (2015).
66. S. L. Wu, W. T. Hu and M. Ma, *Asian J. Chem.*, **25**, 2474 (2013).
67. T. Wu, J. W. Wan and X. B. Ma, *Chin. J. Catal.*, **36**, 425 (2015).
68. H. Li, Z. Fang and S. Yang, *ACS Sustain. Chem. Eng.*, **4**, 236 (2016).
69. F. C. Zheng, Q. W. Chen, L. Hu, N. Yan and X. K. Kong, *Dalton Trans.*, **43**, 1220 (2014).
70. G. Y. Guo and Y. L. Chen, *J. Mater. Sci.*, **39**, 4039 (2004).
71. A. Mondal and S. Ram, *J. Am. Ceram. Soc.*, **87**, 2187 (2004).
72. A. Mondal and S. Ram, *Ceram. Int.*, **30**, 239 (2004).
73. G. Y. Mao, W. J. Yang, F. X. Bu, D. M. Jiang, Z. J. Zhao, Q. H. Zhang, Q. C. Fang and J. S. Jiang, *J. Mater. Chem. B*, **2**, 4481 (2014).
74. H. P. Peng, R. P. Liang, L. Zhang and J. D. Qiu, *Electrochim. Acta*, **56**, 4231 (2011).
75. W. Li, Q. Deng, G. Fang, Y. Chen, J. Zhan and S. Wang, *J. Mater. Chem. B*, **1**, 1947 (2013).
76. H. X. Guo, Y. F. Lian, L. L. Yan, X. H. Qi and R. L. Smith, *Green Chem.*, **15**, 2167 (2013).
77. W. Hertl, *Langmuir*, **5**, 96 (1989).
78. J. C. Van Der Waal, P. J. Kunkeler, K. Tan and H. Van Bekkum, *J. Catal.*, **173**, 74 (1998).
79. C. F. De Graauw, J. A. Peters, H. Van Bekkum and J. Huskens, *Synthesis*, **10**, 1007 (1994).
80. R. A. W. Johnstone, A. H. Wilby and I. D. Entwistle, *Chem. Rev.*, **85**, 129 (1985).
81. A. Stolle, T. Gallert, C. Schmoger and B. Ondruschka, *RSC Adv.*, **3**, 2112 (2013).
82. D. Wang and D. Astruc, *Chem. Rev.*, **115**, 6621 (2015).

Supporting Information

Selective transformation of biomass-derived 5-hydroxymethylfurfural into 2,5-dihydroxymethylfuran via catalytic transfer hydrogenation over magnetic zirconium hydroxides

Lei Hu†, Mei Yang, Ning Xu, Jiaxing Xu, Shouyong Zhou, Xiaozhong Chu, and Yijiang Zhao

Jiangsu Key Laboratory for Biomass-based Energy and Enzyme Technology, School of Chemistry and Chemical Engineering, Jiangsu Collaborative Innovation Center of Regional Modern Agriculture & Environmental Protection, Huaiyin Normal University, Huaian 223300, China

(*Received 18 July 2017 • accepted 22 August 2017*)

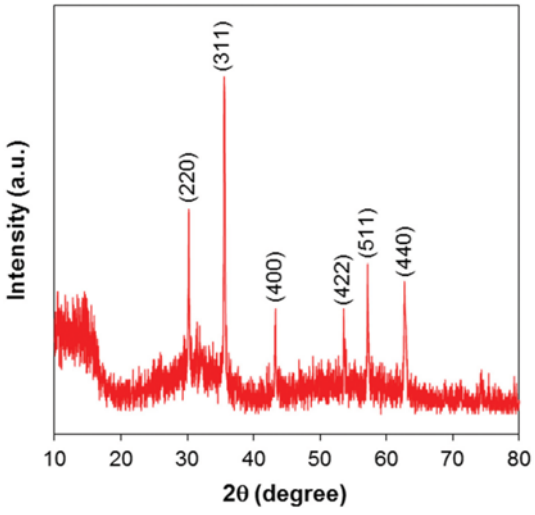

Fig. S1. XRD pattern of Fe_3O_4.

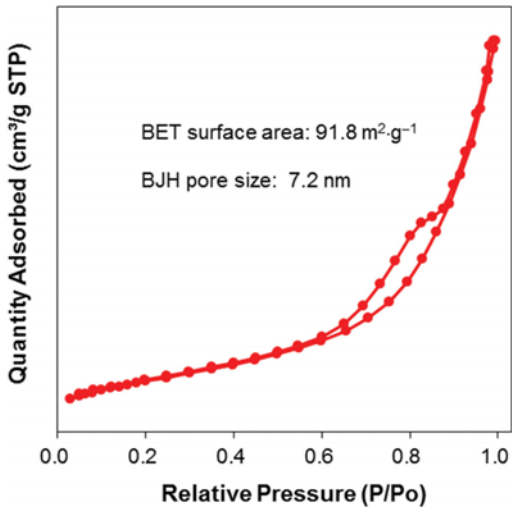

Fig. S2. Nitrogen adsorption-desorption isotherm of Fe_3O_4.

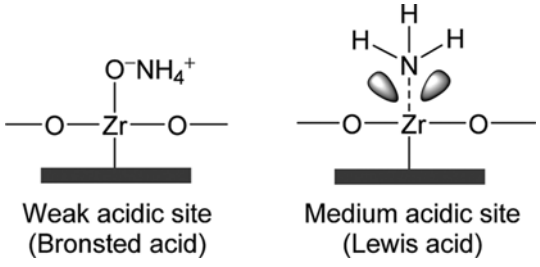

Fig. S3. Two interaction modes of NH_3 with the acidic sites of catalysts.

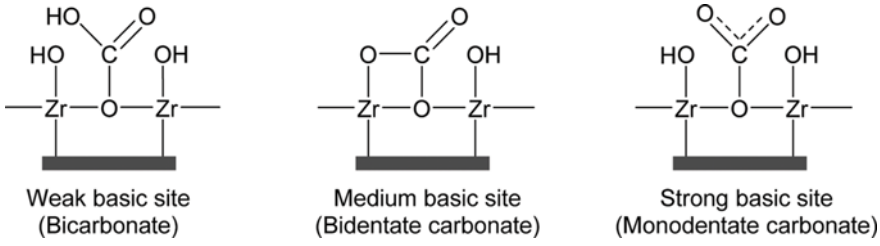

Fig. S4. Three interaction types of CO_2 with the basic sites of catalysts.

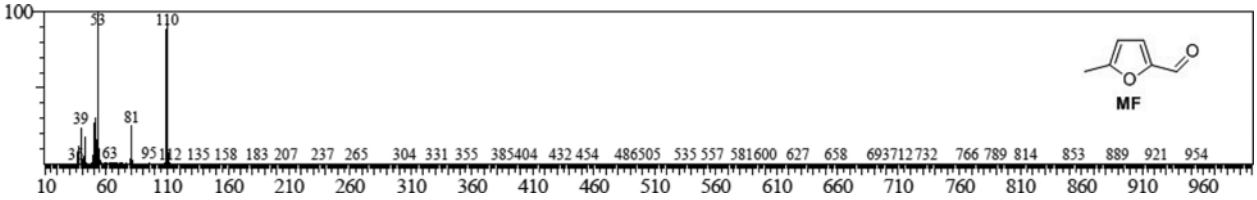

Fig. S5. MS spectrum of MF.

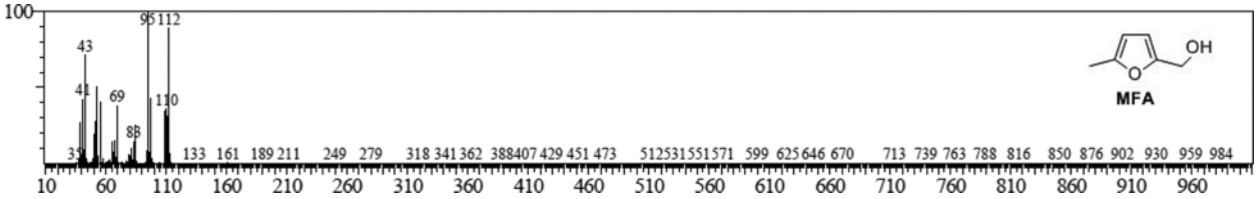

Fig. S6. MS spectrum of MFA.

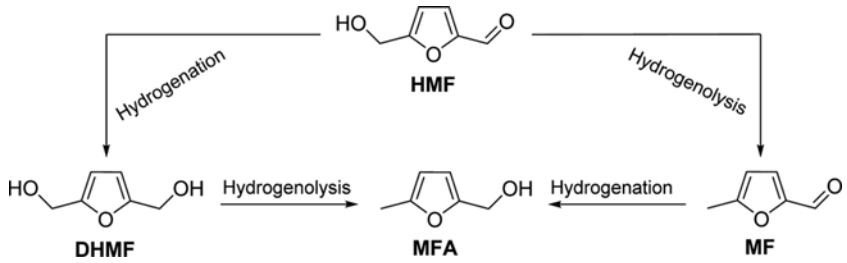

Fig. S7. Hydrogenation and hydrogenolysis of HMF.

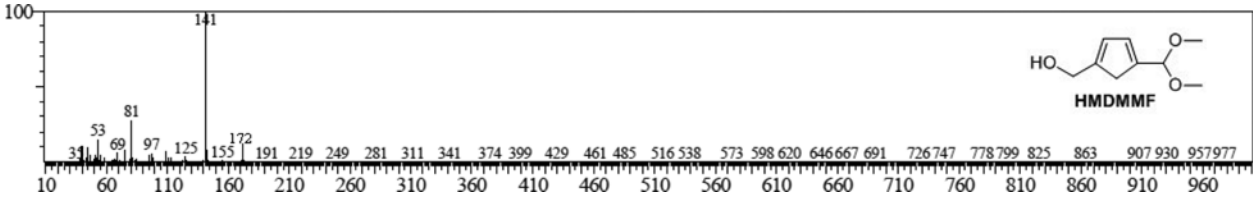

Fig. S8. MS spectrum of HMDMMF.

Table S1. Pore size and acid-base content of MZH(Zr/Fe=2) in the recycling process

Recycle run	Pore size (nm)[a]	Acid content (mmol/g)[b]	Base content (mmol/g)[c]
Fresh	3.1	0.948	1.092
4	2.9	0.903	0.987
Regenerated	3.2	0.926	1.015

[a]Pore sizes were measured by the method of BJH

[b]Acid contents were determined by the profile of NH_3-TPD

[c]Base contents were determined by the profile of CO_2-TPD